MEDIUM ENERGY BEAM TRANSPORT DESIGN UPDATE FOR ESS

I. Bustinduy*, O. González, A. Ghiglino, I. Rodríguez,
J.L. Muñoz, A. Zugazaga, F.J. Bermejo
ESS-Bilbao, Spain
R. Miyamoto, B. Cheymol, M. Eshraqui, J. Stovall
ESS, Sweden

Abstract

The major challenge of this part of the accelerator is to keep a high quality beam, with a pulse well defined in time, a low emittance and a minimized halo, so that the beam losses downstream the linac be limited and the overall ESS reliability be maximized. In order to minimize beam loss at high energy linac, and the consequent activation of components, a fast chopping scheme is presented for the medium energy beam transport section (MEBT). The considered versatile MEBT is being designed to achieve four main goals: First, to contain a fast chopper and its correspondent beam dump, that could serve in the commissioning as well as in the ramp up phases. Second, to serve as a halo scraping section by means of various adjustable blades. Third, to measure the beam phase and profile between the RFQ and the DTL, along with other beam monitors. And finally, to match the RFQ output beam characteristics to the DTL input both transversally and longitudinally. For this purpose a set of ten quadrupoles is used to match the beam characteristics transversally, combined with three 352.2 MHz *buncher* cavities, which are used to adjust the beam in order to fulfill the required longitudinal parameters.

INTRODUCTION

Along the different designs for high-intensity linear accelerators, the MEBT emerges as one of the critical stretches through the accelerator in terms of losses, emittance increase and halo formation. With the purpose of minimizing emittance growth along this section due to the effects of spatial charge, at least the following two conditions must be satisfied: supplying a solid cross focalization and avoiding sharp changes in focalization strength. To this end, a compact quadrupole with a length of 70 mm is being designed. In addition, some of these quadrupoles, whose field gradients vary between 9 and 30 T/m, are expected to incorporate correcting dipoles in order to minimize any beam misalignments (see Table 1).

LAYOUT

The layout (Fig. 1) is being designed to achieve four main goals: First, to contain a fast chopper and its correspondent beam dump, that could serve in the commissioning as well as in the ramp up phases. Second, to serve as a halo scraping section by means of various adjustable blades. Third, to measure the beam phase and profile between the RFQ and the DTL, along with other beam monitors. Finally, to match the RFQ output beam characteristics to the DTL input both transversally and longitudinally. Figure 3 shows the realistic RFQ output distribution used in the simulations, the emittance increase along the MEBT, obtained with TRACEWIN, prior to any collimation scheme is $\Delta\epsilon_{xx'}$=17.2%, $\Delta\epsilon_{yy'}$=14.8%, $\Delta\epsilon_{zz'}=-1.5$%; keeping the halo parameter <1.4 for all planes (see Fig. 2); with a negligible 0.05% of cumulative losses along the line. When the collimation scheme is applied $\Delta\epsilon_{xx'}$=14.1%, $\Delta\epsilon_{yy'}$=10%, $\Delta\epsilon_{zz'}=-1.8$%, while cumulative losses stay below an acceptable 1.3%.

Table 1: MEBT Operation Parameters

Parameter	Value
Input Energy	3 MeV (β =0,0798)
Total Current	50 mA
Particle	protons (H^+)
Number de quadrupoles	10
Min./Max quadrupole gradients	9–30 T/m
Number of *buncher* cavities	3
Frequency	352.2 MHz
Peak power per cavity	14 kW
Effective Voltage (EoTL)	150 kV

The presented layout *S0Q10R3C4*[1] constitutes a relatively compact design (~3600 mm). It comprises a fast chopper structure, beam dump and provides the separation for the required diagnostics. Similarly to CERN, J-PARC and SNS designs, this fast chopper complements to the LEBT pre-chopper, and will be used to sharpen the beam edges produced by the slow-chopper during rising and falling times (~10 ns). Eliminating thus, the partially chopped beam that passes through the RFQ [1]. Fundamentally, the chopping structure is based on the Linac4 design. It consists of an electrostatic traveling wave deflector together with a beam dump for dissipating the sectioned beam current, with the goal of reducing beam losses that will occur at higher energies.

* ibon.bustinduy@essbilbao.org

[1] 0 solenoids, 10 quads, 3 bunchers, 4 collimators

ISBN 978-3-95450-118-2

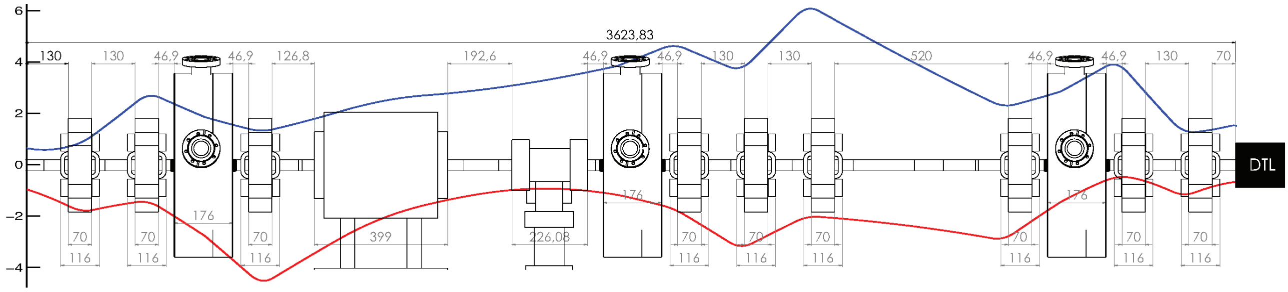

Figure 1: Layout proposed for the ESS MEBT; comprised of 10 quadrupoles 3 bunchers and 3 collimators. *rms* values are also plotted for x (blue) and y (red). All heights are expressed in mm.

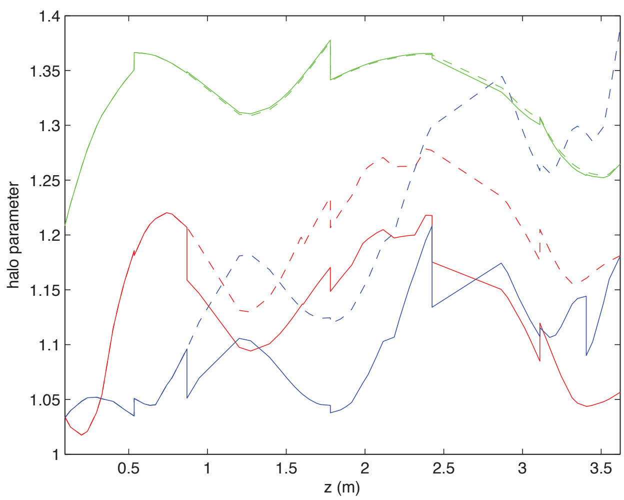

Figure 2: Halo parameters along the line. Red (x), blue (y), and green (z) dashed lines represent halo parameters with no scrapers, while solid lines represent the evolution of the halo components for the collimated beam.

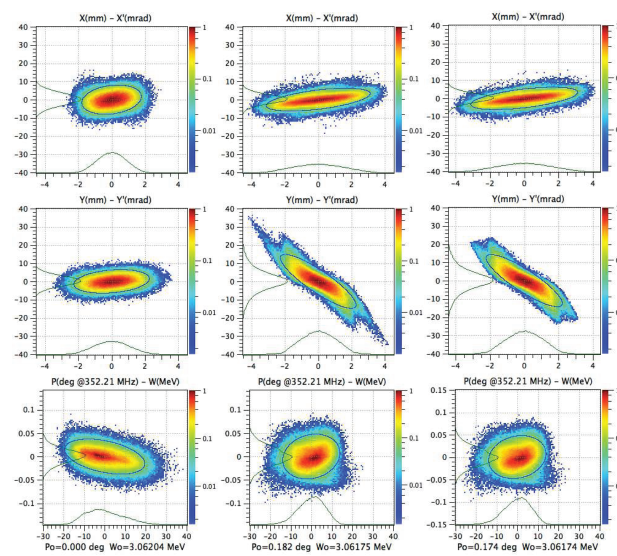

Figure 3: **Left:** Employed RFQ output particle data distribution. Normalized RMS Emittance values at the entrance of the MEBT are: $\epsilon_{xx'}$=0.227, $\epsilon_{yy'}$=0.230, $\epsilon_{zz'}$=0.338 in π.mm.mrad units. **Middle:** Output distribution without any collimation. **Right:** Output distribution with collimation.

Error Study

Magnet translation, rotation and quadrupole gradient errors have been studied, in order to narrow the requirements for the dipolar components needed for the quadrupoles. These steerers (embedded in the Quads) are demanded to correct the beam trajectories from misalignments produced due to manufacture imperfections or alignment errors during the installation phase of the different elements.

Errors have been uniformly distributed; each value expressed in the Table 2 is the maximum range error. Using $\sim 2\times10^5$ particles as input (see Fig. 3). 5 errors steps have taken: [20%, 40%,... 100%]. Once the quadrupole and cavity errors have been introduced for each linac scheme; in each linac tunable parameters are adjusted to maximize transmission maintaining Courant-Snyder parameters at the end of the line. Figure 4 represents the maximum integrated fields required to correct beam trajectories per steerer. This provides the demanded information to close the magnetic design of the quadrupoles.

Table 2: Static Quadrupole and Buncher Errors to be Considered in the MEBT for ESS. The errors are uniformly distributed ($\pm$); each value of the command line is the maximum range error.

Parameter	**Value**
Quadrupole displacement (Δx,Δy)	$\pm$0.5 mm
Quadrupole longitudinal shift (Δz)	$\pm$0 mm
Quadrupole gradient ($\Delta g/g$)	$\pm$1%
Quadrupole rotation (ϕ_x,ϕ_y,ϕ_z)	$\pm 0.1^o$
Cavity displacement (Δx,Δy)	$\pm$0.5 mm
Cavity longitudinal shift (Δz)	$\pm$0 mm
Cavity rotation (ϕ_x,ϕ_y)	$\pm 0.1^o$
Cavity amplitude error ($\Delta E/E$)	$\pm$1%
Cavity phase error ($\Delta\phi/\phi$)	$\pm$1%
Beam Position Monitor	$\pm$0.1 mm

ISBN 978-3-95450-118-2

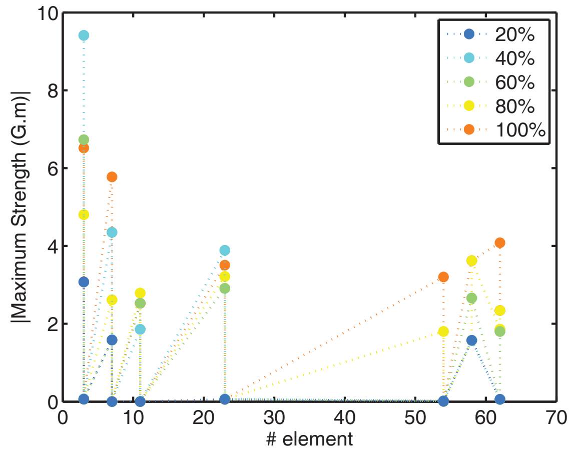

Figure 4: Maximum strength (|G.m|) obtained for each steerer, considering the proposed layout. Results are presented in steps, going from 20% error, 40%, upto 100%.

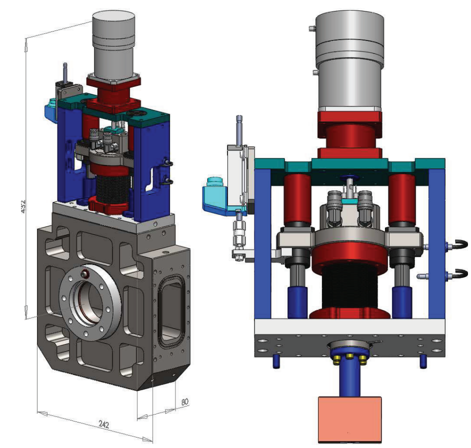

Figure 5: AVS and CIEMAT design for IFMIF scrapers. *Courtesy of I. Podadera and M.A. Carrera.*

Diagnostics

The proposal of ESS beam instrumentation group is to measure the 6D beam phase space in the MEBT using a reducing beam power (100 μs, 50 mA, 1 Hz Rep. rate or 10 μs, 50 mA, 14 Hz Rep. rate) using a list of diagnostics: A set of 6 Beam Position Monitors (BPMs); at least two of those are essential for time-of- flight, three for absolute energy measurement. a Bunch Shape Monitor (BSM) is foreseen for bunch length measurements. One Beam Current Transformers (BCT) will be installed at the beginning. The sampling rate of the BCT shall be 10 MHz with a resolution of 1% of the nominal beam current. A second one will be installed in the DTL tank in order to measure the input current in the DTL. As for the other BCT foreseen to be installed in the warm linac, the current monitors will also measure the beam transmission between two monitors and will be integrated in the Machine Protection System (MPS). 4 Wire Scanners are also, planned to be installed. Two of those wire scanners shall be equipped with high dynamic range electronic in order to measure the beam transverse halo. Finally for emittance measurements, a Slit-and-Grid emittance measurement system is scheduled.

Collimation

The use of scrapers before entering DTL tanks is strongly recommended to avoid emittance growth and halo development in high-intensity linacs [2]. In our current design, collimators should be able to scrap the beam in the both transverse plane at each locations. For this, 4 stepping motors are needed per locations. The scrapper will be used during nominal operation, the collimator system has to be integrated in the interlock system in order to avoid interaction with the beam core, the position of the beam will be provided by a BPM positioned as close as possible to the collimator and the movement has to be limited. In addition, the temperature can be measure in the scrapper and also the charge deposition. CIEMAT/AVS design has been used as a reference for the ESS, see Fig. 5. This scrapper designed for IFMIF (5 MeV, 125 mA, CW, D^+) is made with water refrigerated copper alloy due to the proximity of super conducting structure. In the case of ESS, Carbon/Carbon composite with an additional water cooling system has been considered. A more detailed explanation of the procedure to find the optimum location is given in: [3].

QUADRUPOLE DESIGN

The quadrupoles with integrated steerers for the MEBT cannot be calculated until the optical layout and the mechanical constraints are completely defined. Regarding the optics, the aperture of the quadrupoles must be fixed according to the beam transverse size and maximum losses. The quadrupole gradient and length (or integrated gradient/field) are fixed by the optical focusing requirements, and the dipolar steering strength must be given by the maximum acceptable beam misalignment. The field quality must be defined from optical tracking simulations, and it is especially important for these devices because the steering dipoles are integrated inside the quadrupoles, and that results in a sextupolar component about 30 % of the dipolar steering component ($\sim 50\times10^{-4}$ parts of the main quadrupolar field); to be confirmed by future simulation campaign. Otherwise, independent steerers or embedded $\cos(\theta)$ dipoles will be used. Regarding the mechanical constraints, the maximum distance between quadrupole coil-ends (maximum physical length) is required to design the coil shape and to select a working current density. The minimum distance from the quadrupole to other devices or quadrupoles is also important because the magnetic field can interfere with them and a crosstalk study should be developed. Once all these parameters are defined and fixed, the quadrupole calculation and design can be finished. The preliminary calculations already done for the quadrupoles are based on the following preliminary

ISBN 978-3-95450-118-2

Table 3: Computed Figures of Merit for the Optimized *A30W126T45v1*. Results for the CERN and FETS cavities are also presented.

Model	ESS	CERN B30	FETS
Freq, [MHz]	352.20	357.22	315.86
Q_0	23477	24129	27222
T	0.593	0.56	0.636
V_0T, [kV]	140	140	160
P, [kW]	14.02	15.38	11.82
r, [MΩ]	1.4	1.27	2.35
ZT^2, [MΩ/m]	11.1	10.11	15.67
$E_{s,max}$, [MV/m]	27.2	24.25	27.56
Kilpatrick (b)	1.47	1.3	1.49

specifications: 34 mm aperture, 20 T/m with 70 mm effective length, 116 mm maximum physical size (length) and 1.5 mrad (∼4 G.m) deflection for the steerers. Using these values, a preliminary model has been developed (see Fig. 8)

BUNCHER CAVITIES

The buncher design is an iterative process between the electro-magnetic, thermo-mechanic, RF and beam dynamics groups, which also affects the tuner and coupler design.

Electromagnetic Design

When designing the cavity, a high shunt impedance per unit length ZT^2 is desirable in order to reduce the power consumption and therefore to simplify the cooling system. Nevertheless, electrical discharges must be avoided by limiting the peak surface electric fields. Using a stochastic hill-climbing and a genetic algorithm implementation [4], the *A30W126T45v1* model was considered as the best compromise. Table 3 summarizes the parameter list of the current Electro-Magnetic design [5].

Tuning System

A study on the tuning system required for the bunching cavity in order to correct the frequency shift due to both the thermal expansion and the manufacturing tolerances was also done. The insertion in the cavity of a plunger tuner in a region of high magnetic field increases the resonant frequency of the TM_{010} accelerating mode. In this study, one and two hollow cylinders were inserted into the cavity in different positions and different penetration levels. In latter configuration, a tuning range of almost 2 MHz was obtained, thus doubling the range obtained with only one tuner. In addition, the E_z field along the axis of the cavity was not affected by the presence of the tuners. Finally, we confirmed that the resonant frequency of the cavity is barely dependent on the relative positions of the tuners [6].

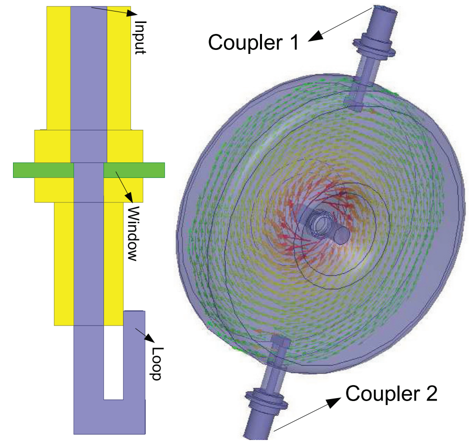

Figure 6: **Left:** Electromagnetic model of the drum-like coupler including the coupling loop designed for the cavity. **Right:** Magnetic field intensity H_θ of the TM_{010} mode resonating in the cavity induced by the power couplers.

Power Coupler

The purpose of the power coupler is to inject the RF power into the re-bunching cavities. The couplers have also to protect the vacuum of the cavities. This is usually obtained by using a RF ceramic window.

The designed model for the coupler contains two additional transitions to the input, output, and window coaxial. Each transition is located at one side of the ceramic window. Thus, by changing the dimensions of the transitions (both length and radius) and the window (radius), the required matching can be obtained.

The final dimensions for the input and output flanges will be fixed when the mechanical design of the coupler will be addressed. The coupler under study was designed and analyzed by a Full-Wave electromagnetic simulator. The input and output coaxial dimensions for the electromagnetic design, chosen to guarantee a characteristic impedance of Z_0=50 Ω. Those dimensions have been taken as a reference from the coupler of the linac4 *chopper line* buncher. Nevertheless, those dimensions can be changed, if required. The ceramic window of the ESS MEBT coupler has been fixed as a cylinder with L_{window}=6 mm. However, this value can be modified on demand.

Once the window transitions of the coupler have been designed, a loop is added to the model. This loop must inductively couple the power coming from the RF distribution system into the re-bunching cavity (see Fig. 6). This coupling is directly related to the area covered by the loop which ensures the minimum magnetic flux needed [7].

Thermo-mechanical Design

Once the actual heat deposition is obtained from EM calculations, the heat flux deposition can be coupled with FLUENT using a UDF (User-Defined Function). This file contains the heat flux applied to all zones of the buncher

ISBN 978-3-95450-118-2

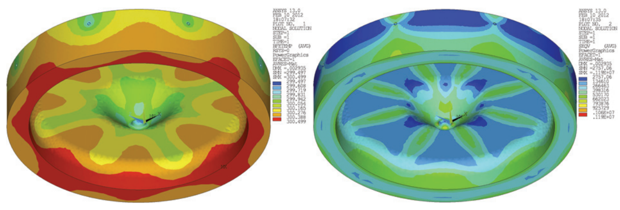

Figure 7: Ansys temperature (left) and stress (right) fields.

Cavity, where the maximum value is reached at the *nose* of the geometry. After using the UDF to apply the heat flux to the geometry, FLUENT is launched to solve the Computational Fluid Dynamics problem iteratively. For a 1.4 kW average power for the cavity[2], the temperature increase reached at the *nose* is around 2 ^{o}C, while the rest of the solid has an homogeneous temperature and its value is between 300-300.5 K (see Fig. 7). A water mass flow rate of 0.077 kg/s is circulated inside each channel (Ø7 mm), reaching 3.6 m/s after the elbow. The average velocity in the rest of the flow is around 2.16 m/s [8].

Once the thermal hydraulic analysis is finished and the temperature field is obtained, a thermo-mechanical analysis can be performed coupling FLUENT with ANSYS. The most important results obtained from the thermo-mechanical analysis are the stress and strain values, because these parameters are material and geometrical restrictions respectively. Stress field is around 1.2 MPa near channels zones (see Fig. 8). This is a very low value and it is significantly lower than the yield strength of the material (around 270 MPa for oxygen-free tempered copper) and the fatigue strength also (115 MPa for treated copper working 300×10^6 cycles). Finally, maximum strain values for x,y and z coordinates are 0.005, located in the *nose*, where temperature is higher [9].

Manufacturing Considerations

The cavity mechanical design comprises two main pieces: one includes the cavity barrel and one cover, while the other piece includes only one cover. Each piece will be made in SS (AISI304), after the machining the commercial flanges will be welded to the body. Once all the components of the cavity are assembled the interior of the 2 pieces will be copper plated 30 μm, creating a layer thick enough for the RF requirements. Both parts will be assembled using an HELICOFLEX© Metal Seals to guarantee the vacuum requirements. This model is fabricated with all the ports opened and the tuners (one fixed and one movable) in the right positions. The assembled cavity is then measured to verify the design and to check the resonant frequency. Afterwards, the cover piece edge is machined, so when the full cavity is assembled the gap length would be smaller (resulting in lower resonant frequency). This process continues until the desired frequency is obtained.

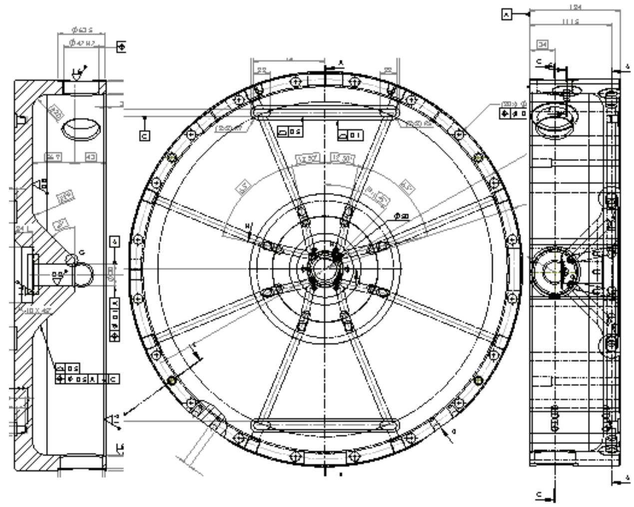

Figure 8: Engineering detail of the *A30W126T45v1* buncher cavity drawings with its characteristic Maltese cross shape cooling channels.

The movable tuner range must be sufficient to deal with the frequency shift due to the thermal expansion of the cavity, which mainly appears on the nose cones of the gap area. Therefore, during operation, the cavity geometry will be very similar to the one obtained by optimizing the geometry at 352.2 MHz.

[2] 35 kW peak power for a 4% duty, giving thus a 2.5 safety factor respect to the simulated dissipated power on the walls. See Table 3.

REFERENCES

[1] J.B. Lallement, "Pre-Chopper Beam Dynamics", CERN Linac4 Internal Report, 2010.

[2] F Gerigk, et al., "High Current Linac Design with Examples of Resonances and Halo", Proc. XXI International Linear Accelerator Conference (LINAC 2002), Gyeongju, Korea, 19-23 Aug 2002

[3] R. Miyamoto, et al., "Beam Loss and Collimation in the ESS Linac", WEO3A02, these proceedings.

[4] J.L. Munoz, I. Rodriguez, "Multiphysics Design of ESS-Bilbao Linac Accelerating Cavities", COMSOL Conference 2011, Stuttgart.

[5] O. Gonzalez et al., "Preliminary Electromagnetic Design of the Re-bunching RF Cavities for the ESS MEBT", ESS AD Technical Note, (ESS/AD/0036)

[6] O. Gonzalez et al., "Electromagnetic Design of the Tuning System for the Re-bunching Cavities of the ESS MEBT", ESS AD Technical Note, (ESS/AD/0035)

[7] O. Gonzalez et al., "Electromagnetic Design of a Power Coupler for the ESS MEBT", *Internal Report*.

[8] A.Ghiglino, et al., "Rebunching Cavity: Preliminary Design Report", ESS AD Technical Note, (ESS/AD/0037).

[9] A.Ghiglino, et al., "Rebunching Cavity: Results of First Iteration with Real Heat Generation", ESS AD Technical Note, (ESS/AD/0038).

ISBN 978-3-95450-118-2